

STRONG COUPLING BETWEEN A PERMALLOY FERROMAGNETIC CONTACT AND HELICAL EDGE CHANNEL IN A NARROW HgTe QUANTUM WELL

A. Kononov^a, S. V. Egorov^a, Z. D. Kvon^{b,c},
N. N. Mikhailov^b, S. A. Dvoretsky^b, E. V. Deviatov^{a}*

^a Institute of Solid State Physics, RAS
 142432, Chernogolovka, Moscow Region, Russia

^b Institute of Semiconductor Physics
 630090, Novosibirsk, Russia

^c Novosibirsk State University
 630090, Novosibirsk, Russia

Received June 14, 2016

We experimentally investigate spin-polarized electron transport between a permalloy ferromagnet and the edge of a two-dimensional electron system with band inversion, realized in a narrow, 8 nm wide, HgTe quantum well. In a zero magnetic field, we observe strong asymmetry of the edge potential distribution with respect to the ferromagnetic ground lead. This result indicates that the helical edge channel, specific for the structures with band inversion even at the conductive bulk, is strongly coupled to the ferromagnetic side contact, possibly due to the effects of proximity magnetization. This allows selective and spin-sensitive contacting of helical edge states.

DOI: 10.7868/S0044451016110000

1. INTRODUCTION

Recently, there is a strong interest in two-dimensional semiconductor systems with an inverted band structure, like narrow HgTe quantum wells. This interest is mostly connected with the quantum spin Hall (QSH) effect regime [1, 2]. Similarly to the conventional quantum Hall (QH) effect in high magnetic fields [3], QSH regime is characterized [4, 5] by presence of two spin-resolved, current-carrying helical edge states [6–9] even in a zero magnetic field. The helical QSH edge states are regarded to be suitable for different applications like quantum computing and cryptography.

Experimental investigations of helical QSH edge states are mostly based on charge transport along the edge, which has been detected in local and nonlocal resistance measurements [1, 2, 4, 5] and by a direct visualization technique [10]. In the last case, the edge

current has even been demonstrated to coexist with the conductive bulk [10], which is also possible from theoretical considerations [6, 11]. Despite the initial idea of a topological protection [1, 7–9], backscattering appears at macroscopic distances [2, 5], possibly due to the allowed two-particle process [12] or the electron puddles [13].

It is clear that for possible applications, it is necessary to develop a technique of selective contacting of these edge states. A possible variant is to use spin effects: QSH edge transport is supposed to be essentially spin-dependent [6–9] even in a zero magnetic field. Strong coupling between the spin-resolved helical edge states and a ferromagnet can also be anticipated from theoretical considerations [14, 15].

Here, we experimentally investigate spin-polarized electron transport between a permalloy ferromagnet and the edge of a two-dimensional electron system with band inversion, realized in a narrow, 8 nm wide, HgTe quantum well. In a zero magnetic field, we observe strong asymmetry of the edge potential distribution with respect to the ferromagnetic ground lead. This result indicates that the helical edge channel, specific

* E-mail: dev@issp.ac.ru

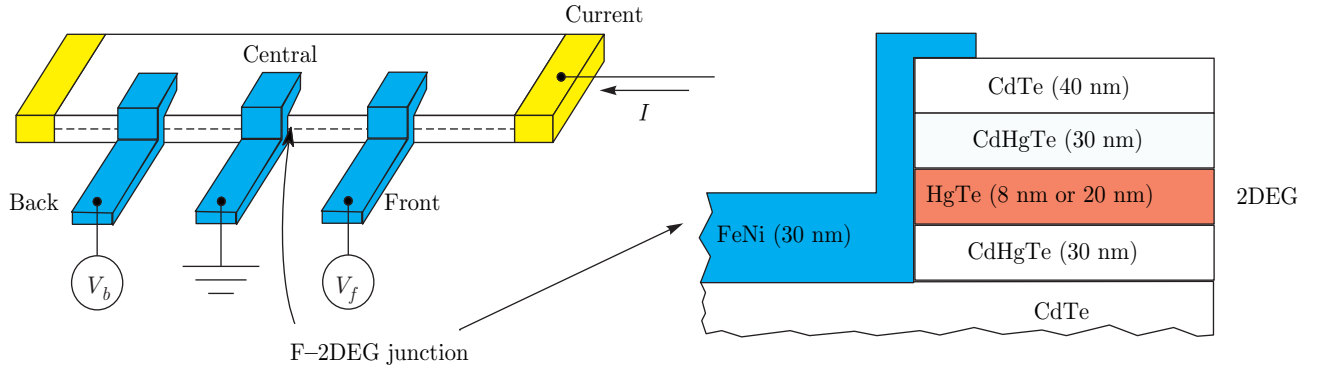


Fig. 1. (Color online) Sketch of the type-A sample (not in scale) with electrical connections. Three ferromagnetic permalloy $\text{Fe}_{20}\text{Ni}_{80}$ stripes (denoted as front, central, and back) are placed at the 200 nm mesa step, with a small (2–3 μm) overlap. The width of each stripe is equal to 20 μm . They are separated by a 100 μm distance along the sample edge. In every overlap region, a side junction is formed between the ferromagnetic lead and the 2DEG edge. We study electron transport through the F–2DEG interface in a standard three-point technique: the central ferromagnetic electrode is grounded; a current is applied between it and one of the normal Au (yellow) contacts; two other ferromagnetic electrodes trace the 2DEG potential to both sides of the grounded junction, V_f and V_b

for the structures with band inversion even at the conductive bulk, is strongly coupled to the ferromagnetic side contact, possibly due to the effects of proximity magnetization. This allows selective and spin-sensitive contacting of helical edge states.

2. SAMPLES AND TECHNIQUE

Our $\text{Cd}_{0.65}\text{Hg}_{0.35}\text{Te}/\text{HgTe}/\text{Cd}_{0.65}\text{Hg}_{0.35}\text{Te}$ quantum wells are grown by molecular beam epitaxy on GaAs substrate with [013] surface orientations. The layer sequence is shown in Fig. 1; a detailed description can be found elsewhere [16, 17]. Our wells are characterized by band inversion [2, 5], because the well width $d = 8$ nm is above the critical value 6.3 nm. They contain a 2DEG with the electron density $1.5 \cdot 10^{11} \text{ cm}^{-2}$, as obtained from standard magnetoresistance measurements. The 2DEG mobility at 4 K equals $2 \cdot 10^5 \text{ cm}^2/\text{V}\cdot\text{s}$. For samples with higher $d = 20.5$ nm, a 2D system in the quantum well represents an indirect 2D semimetal [18, 19]. Both electrons and holes contribute to transport in this case. The carrier concentrations are low enough, about $0.5 \cdot 10^{11} \text{ cm}^{-2}$ and $1 \cdot 10^{11} \text{ cm}^{-2}$ for electrons and holes, respectively. The low-temperature mobility of electrons is about $4 \cdot 10^5 \text{ cm}^2/\text{V}\cdot\text{s}$, because the holes (with a lower mobility of $5 \cdot 10^4 \text{ cm}^2/\text{V}\cdot\text{s}$) provide efficient disorder screening [20].

Our principal idea is to use the side contact to the 2DEG edge at the mesa step [21–23]. Indeed, the usual procedure with annealed In contacts is not se-

lective with respect to the edge state transport. Annealed In provides high-quality Ohmic contact primary to the bulk 2DEG. Thus, although the edge current is allowed [6, 11] to coexist with the conductive bulk [10], edge state transport can only be investigated near the charge-neutrality point [1, 2, 4, 5]. In contrast, without an annealing procedure, the side contact is coupled to the 2DEG edge at the mesa step, because the CdTe layer on the top of the structure is a high-quality insulator at low temperatures.

A sample sketch is presented in Fig. 1. The mesa 100 μm wide is formed by dry etching (200 nm deep) in Ar plasma. We fabricate F–2DEG junctions by using rf sputtering to deposit 50 nm thick ferromagnetic permalloy $\text{Fe}_{20}\text{Ni}_{80}$ stripes at the mesa step, with a small (2–3 μm) overlap. The stripes are formed by the lift-off technique, and the surface is mildly cleaned by Ar plasma before sputtering. To avoid any 2DEG degradation, the sample is not heated during the sputtering process. The source-drain contacts (yellow in Fig. 1) are obtained by thermal evaporation of 100 nm thick Au, as well as the normal Au–2DEG side junctions for reference samples.

We study electron transport across one particular F–2DEG junction in a three-point technique represented in Fig. 1: the central ferromagnetic electrode is grounded; a current is applied between it and one of the normal contacts (source or drain); and two other permalloy contacts (front and back) trace the 2DEG potential to both sides of the grounded junction, V_f and V_b .

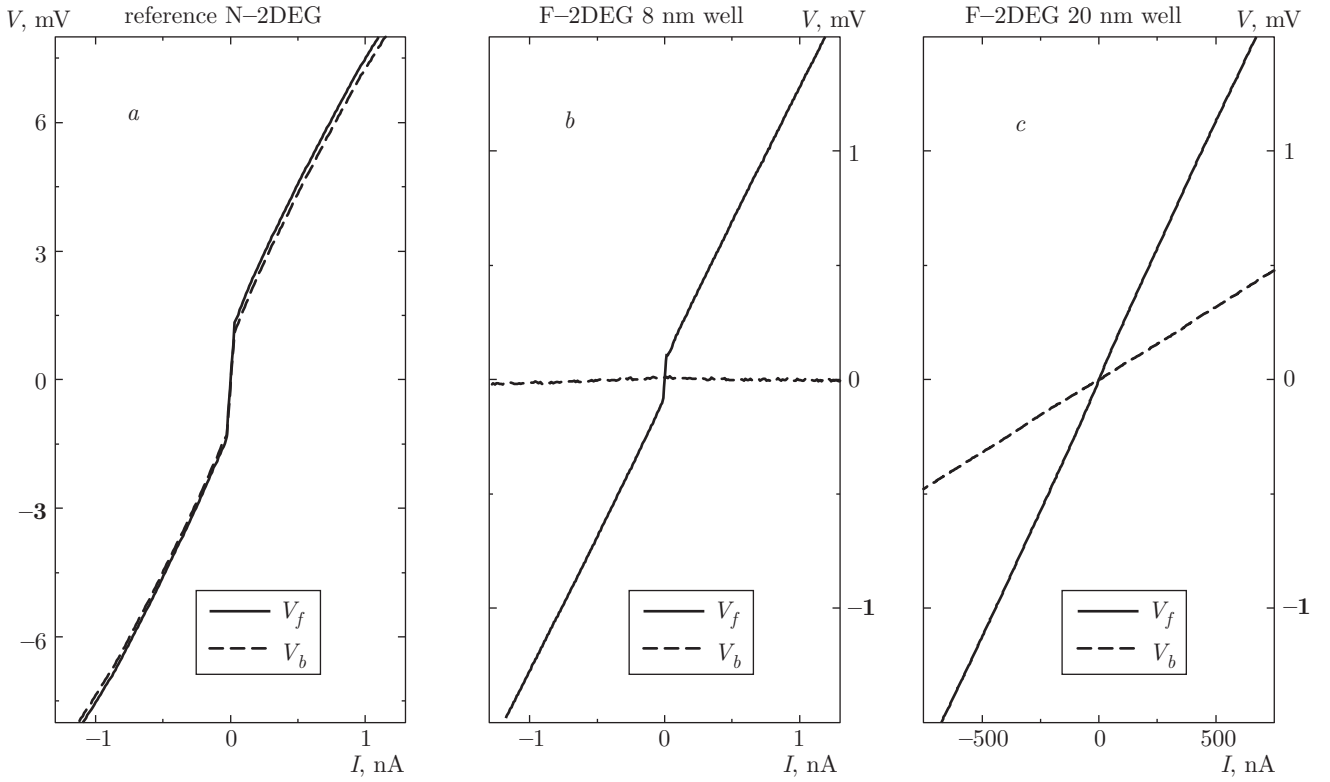


Fig. 2. Examples of I - V characteristics for transport across a single (a) normal N-2DEG or (b,c) ferromagnetic F-2DEG junction. The measurements are performed at a temperature of 30 mK in a zero magnetic field. (a) For a reference sample with Au-2DEG junctions, V_f and V_b coincide well and reflect the resistance of the N-2DEG interface in a standard three-point configuration. (b) For the ferromagnetic F-2DEG junction to the 8 nm HgTe quantum well, we obtain a significant signal V_f , but V_b is always zero. (c) For the 20 nm HgTe quantum well, V_f and V_b are different, but they are of the same order of magnitude: we do not observe $V_b = 0$ in this case. The data for the 8 nm HgTe quantum well (b) indicate perfect coupling of the grounded ferromagnetic electrode to the conductive edge channel

We sweep the dc current and measure voltages in the mV range by a dc electrometer. The resulting I - V characteristics are presented in Figs. 2 and 3. To obtain $dV/dI(V)$ characteristics in Fig. 5 (see below), this dc current is additionally modulated by a low ac component (0.01 nA, 2 Hz). We measure the ac (proportional to dV/dI) component of the 2DEG potential by using a lock-in with a 100 M Ω input preamplifier. We have verified that the lock-in signal is independent of the modulation frequency in the range 1–6 Hz, which is defined by the applied ac filters.

The measurements are performed at a temperature of 30 mK. To realize spin-polarized transport, the permalloy stripes are initially pre-magnetized in the 2DEG plane [21]. The sample is placed within a superconducting solenoid, such that the initial in-plane magnetization can be changed by introducing a relatively high (above 1 T) external magnetic field. The field is switched to zero afterwards and the measurements are performed in the zero magnetic field.

Qualitatively similar results were obtained from different samples in several cooling cycles. We study several samples of the type A (from both 8-nm and 20-nm HgTe quantum wells), which are depicted in Fig. 1, and one of the type B, which is additionally covered by a metallic Al gate. The gate covers the entire sample (bulk 2DEG, mesa edges, all F-2DEG junctions), except the normal Ohmic contacts. To avoid gate leakage, the Al gate is placed over a 350 nm thick dielectric (guanine) layer. We verified that there is no noticeable gate leakage through the dielectric at ± 5 V dc gate bias. As a reference, we use a sample with Au (normal) side junctions instead of the permalloy ones.

3. EXPERIMENTAL RESULTS

Examples of I - V characteristics are presented in Fig. 2 for transport across a single normal N-2DEG or ferromagnetic F-2DEG junction.

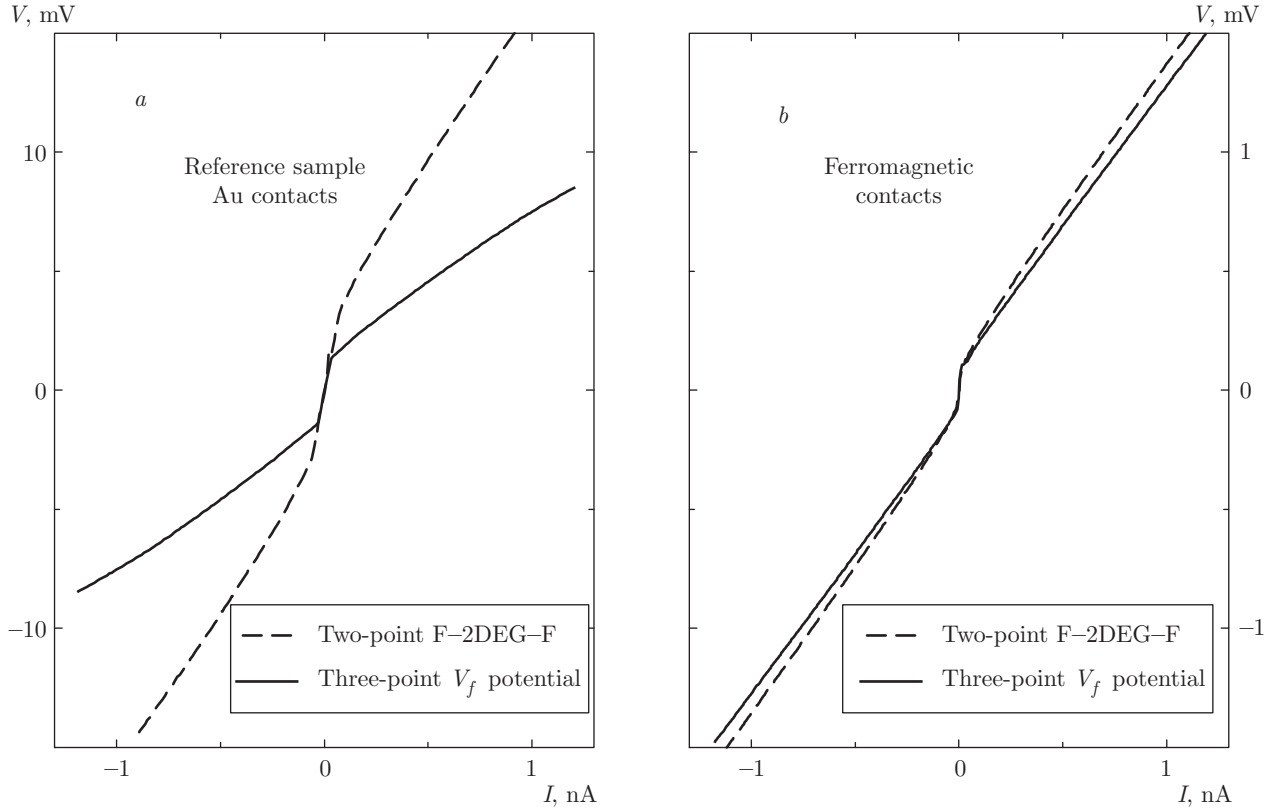


Fig. 3. Two-point I - V characteristics (dash) for (a) double normal Au-2DEG-Au or (b) ferromagnetic F-2DEG-F junctions in comparison with the three-point potential V_f from Fig. 2a and b. The experimental Au-2DEG-Au I - V dependency reflects the resistance of two mostly identical Au-2DEG interfaces. In contrast, the two-point F-2DEG-F curve coincides well with the three-point V_f potential, and therefore reflects the resistance of the edge channel with negligible interface contributions. The measurements are performed at a temperature of 30 mK in the zero magnetic field for the 8 nm wide HgTe well sample

In a three-point technique, the measured potential V reflects in-series connected resistances of the grounded contact and the 2DEG. This technique is especially convenient if the first term is dominant. In this case, the 2DEG is equipotential, and therefore the measured three-point I - V curve is independent of the particular positions of the current/voltage probes.

This is exactly what we have for the reference normal Au-2DEG junction shown in Fig. 2a. The I - V curves coincide well for both potential probes V_f and V_b . The measured three-point I - V curves in Fig. 2a reflect the behavior of the (grounded) Au-2DEG interface. These I - V curves are obviously nonlinear and are characterized by a high resistance (about $10 \text{ M}\Omega$) in Fig. 2a. The low-current resistive region with two kinks at about ± 1.5 mV indicates a significant potential barrier (depletion region [24,25]) at the 2DEG edge. Similar high-resistive junctions were obtained for other nonmagnetic materials like sputtered Nb and NbN [22].

Our most prominent experimental result is demonstrated in Fig. 2b. If we ground the permalloy ferromagnetic side contact to the 8 nm HgTe quantum well, as depicted in Fig. 1, the measured potential is strongly asymmetric. We obtain a significant signal V_f (for the voltage probe placed between the current and ground ones), but V_b is always zero. We also observe the same behavior for both current polarities for two different current probes in Fig. 1, and hence the asymmetry between V_f and V_b is not connected with any absolute direction in the sample. This asymmetry is only determined by the mutual positions of the current and voltage contacts with respect to the grounded ferromagnetic lead. Identical behavior is obtained for different ferromagnetic contacts and different 8 nm well samples. We emphasize that the behavior depicted in Fig. 2b is very unusual and is in high contrast to the standard three-point resistance of a reference Au contact in Fig. 2a.

The asymmetry $V_f \gg V_b = 0$ cannot originate from the bulk 2DEG contribution to the measured potential: different signals $V_f > V_b$ would require the bulk 2DEG resistance to strongly exceed the F–2DEG interface contribution. Because of high-resistive curves in Fig. 2b (about $1 \text{ M}\Omega$ corresponding resistance), this is inconsistent with the metallic bulk conductivity (below $1 \text{ k}\Omega$) at the electron concentration $1.5 \cdot 10^{11} \text{ cm}^{-2}$ in our samples.

To verify this conclusion experimentally, similar measurements are performed for a 20 nm wide HgTe quantum well, see Fig. 2c. In this case, V_f and V_b are also different but they are of the same order of magnitude: we do not observe $V_b = 0$ in this case. Both experimental I – V curves correspond to the resistance about $1 \text{ k}\Omega$, which is comparable with the bulk values. In other words, Fig. 2c experimentally demonstrates a typical effect of the bulk current contribution to a three-point signal in the case of low F–2DEG interface resistance.

The only difference between 8 nm and 20 nm HgTe quantum wells is the conductive helical edge channel in the former case [4, 5]. From the continuous evolution of the edge current when the system is being driven away from the charge-neutral regime, demonstrated in Ref. [10] by a direct visualization experiment, we can reasonably suppose that the edge current is still carried by helical spin-resolved edge states even at the conductive bulk 2DEG. This requires low coupling between the edge states and the bulk, possibly because of the formation of a depletion region where the edge channel is laterally localized [10]. The depletion region of a finite width is often present at the 2DEG edge due to electrostatic effects [24, 25]. This depletion region is also confirmed in our experiment by the fact that $V_b = 0$ for any distance to the potential probe in Fig. 2b.

Because the conductive channel is present at the edge of a 8 nm HgTe quantum well, the perfect asymmetry ($V_b = 0$ for any current I) of the edge potential $V_f \gg V_b$, observed in Fig. 2b, indicates that the grounded ferromagnetic side electrode is perfectly coupled to this channel.

We verify the statement of ideal coupling of the ferromagnetic lead to the edge current by a standard two-point characterization, shown in Fig. 3. It can be seen that the two-point F–2DEG–F I – V curve measured between two neighboring ferromagnetic contacts coincides well with the three-point V_f potential in Fig. 2b, and therefore the interface contribution is negligible. In contrast, the experimental Au–2DEG–Au I – V curve in Fig. 3a corresponds to a roughly two times higher resistance than three-point potentials V_f and V_b in Fig. 2a,

and it therefore mostly reflects the resistance of two resistive Au–2DEG interfaces.

4. DISCUSSION

We conclude that only a ferromagnetic permalloy side contact is strongly coupled to the conductive helical edge channel in a zero magnetic field: (i) the perfect asymmetry ($V_b = 0$ for any current I) of the edge potential $V_f \gg V_b$ (see Fig. 2b) is only observed for the 8 nm quantum well; (ii) the coincidence between the two-point F–2DEG–F I – V curve with the three-point V_f potential (see Fig. 3b) directly indicates negligible F–2DEG interface contributions.

If the transport current is concentrated at the edge, it flows along the shortest edge to the ground lead, and there should be no current flowing near the potential probe V_b , and therefore $V_b = 0$ for any current I . The potential V_f in Fig. 2b therefore reflects solely the resistance of the edge channel between two ferromagnetic contacts. It corresponds to the resistance of about $1 \text{ M}\Omega$, which is also well known for the transport along helical current-carrying states at macroscopic distances [5]. It is worth to mention that this $1 \text{ M}\Omega$ resistance is still much smaller than the resistance for transport through the edge depletion region to the bulk (cf. Fig. 2a), and therefore the edge channel is still decoupled from the bulk even at macroscopic distances.

This strong coupling is not defined by chemical composition of the metallic film or the fabrication technique: the sputtered permalloy film contacts the 20 nm

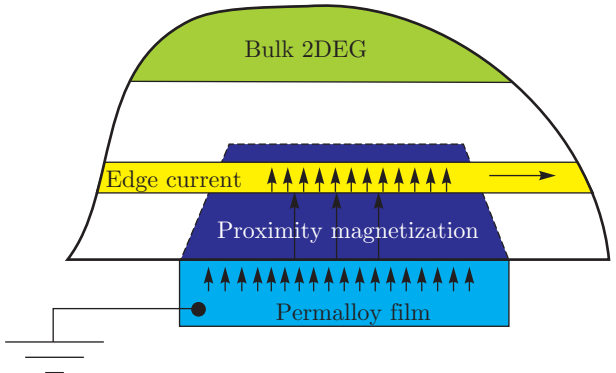


Fig. 4. (Color online) Top view of the 2DEG near the ferromagnetic contact. A depletion region (white) is shown where the edge current is laterally localized (yellow region). A blue region, surrounded by the dashed line, schematically depicts a vicinity of the contact where the proximity magnetization is important. Here, spin-polarized transport couples the edge current to the ferromagnetic side contact

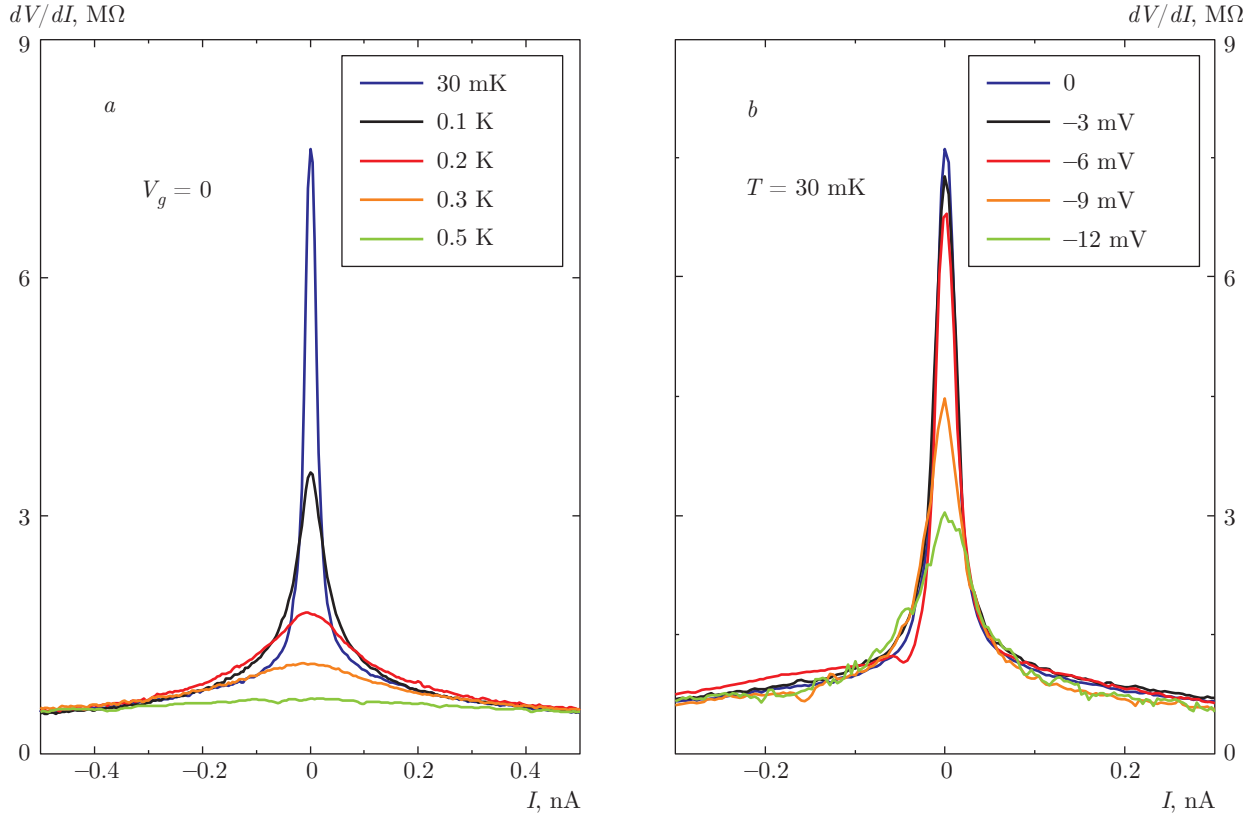


Fig. 5. (Color online) Differential resistance dV_f/dI at low currents. The zero-bias resistance peak is strongly affected by (a) temperature and (b) gate voltage. It disappears completely above 0.5 K , which is consistent with the nonlinearity onset at approximately 0.06 mV in Fig. 2b. The measurements are performed in the zero magnetic field for the 8 nm wide HgTe well sample B with a metallic gate

HgTe quantum well similarly to other nonmagnetic materials. There should be a specific magnetic (spin-dependent) process that couples the spin-polarized ferromagnetic side contact and the one-dimensional helical channel at the edge of a 2DEG with band inversion: a proximity magnetization locally aligns [14,15] the spins of two helical edge states in the vicinity of the ferromagnetic contact. The spin-polarized electron flow from the ferromagnetic contact can be easily injected to the helical state with the corresponding spin projection. The depletion at the interface decouples the bulk 2DEG and makes the helical edge mode even more important. Further transport along the sample edge is diffusive at macroscopic distances [2,5] because of allowed backscattering [12,13] with the injected electrons flowing along the shortest edge to the ground lead. The coupling is independent of the magnetization direction, as we observe in the experiment, because it is the contact magnetization that defines the spin alignment direction (see Fig. 4).

Proximity magnetization can be directly identified in the experimental data. It opens a gap in the one-

dimensional spectrum in the vicinity of the contact [15], which can be seen in Fig. 2b as a high-resistance region approximately 0.06 mV in width. This gap only affects the edge channel resistance and has no effect on its coupling to the ferromagnetic electrode.

The zero-bias resistive region is demonstrated in detail in Fig. 5 as $dV/dI(I)$ dependences for the sample B with a metallic gate. It disappears completely above 0.5 K , which is consistent in value with the nonlinearity onset of about 0.06 mV in Fig. 2b. In contrast, the linear branches of the $dV/dI(I)$ – I curve are invariant below 1 K , which is also consistent with the reported temperature behavior of the diffusive helical edge state transport at macroscopic distances [26]. The zero-bias resistive region is strongly sensitive to the gate voltage, even though it is low enough to have no effect on the bulk carrier concentration (see Fig. 5b). The suppression is fully symmetric with respect to the gate voltage sign. We relate this to the edge state structure reconstruction [15] in the vicinity of a ferromagnetic contact (denoted by a blue region in Fig. 4), which, however, needs further investigations. A magnetic field above

0.2 T sharply increases the zero-bias resistive region. This behavior is consistent with a spectrum gap [15] due to proximity magnetization; the gap value can be estimated as approximately 0.06 meV.

5. CONCLUSION

We experimentally investigated spin-polarized electron transport between a permalloy ferromagnet and the edge of a two-dimensional electron system with band inversion, realized in a narrow, 8 nm wide, HgTe quantum well. In the zero magnetic field, we observe strong asymmetry of the edge potential distribution with respect to the ferromagnetic ground lead. This result indicates that the helical edge channel, specific for the structures with band inversion even at the conductive bulk, is strongly coupled to the ferromagnetic side contact, possibly due to the effects of proximity magnetization. It allows selective and spin-sensitive contacting of helical edge states.

We wish to thank V. T. Dolgopolov, V. A. Volkov, I. Gornyi, and T. M. Klapwijk for fruitful discussions. We gratefully acknowledge financial support by the RFBR, RAS, and the Ministry of Education and Science of the Russian Federation under Contract No. 14.B25.31.0007.

REFERENCES

1. M. König, S. Wiedmann, C. Brüne, A. Roth, H. Buhmann, L. W. Molenkamp, X.-L. Qi, and S.-C. Zhang, *Science* **318**, 766 (2007).
2. G. M. Gusev, Z. D. Kvon, O. A. Shegai, N. N. Mikhailov, S. A. Dvoretsky, and J. C. Portal, *Phys. Rev. B* **84**, 121302(R) (2011).
3. M. Büttiker, *Phys. Rev. B* **38**, 9375 (1988).
4. A. Roth, C. Brüne, H. Buhmann, L. W. Molenkamp, J. Maciejko, X.-L. Qi, and S.-C. Zhang, *Science* **325**, 294 (2009).
5. G. M. Gusev, E. B. Olshanetsky, Z. D. Kvon, O. E. Raichev, N. N. Mikhailov, and S. A. Dvoretsky, *Phys. Rev. B* **88**, 195305 (2013).
6. B. A. Volkov and O. A. Pankratov, *Pis'ma v Zh. Eksp. Teor. Fiz.* **42**, 145 (1985).
7. S. Murakami, N. Nagaosa, and S.-C. Zhang, *Phys. Rev. Lett.* **93**, 156804 (2004).
8. C. L. Kane and E. J. Mele, *Phys. Rev. Lett.* **95**, 146802 (2005).
9. B. A. Bernevig and S.-C. Zhang, *Phys. Rev. Lett.* **96**, 106802 (2006).
10. K. C. Nowack, E. M. Spanton, M. Baenninger, M. König, J. R. Kirtley, B. Kalisky, C. Ames, P. Leubner, C. Brüne, H. Buhmann, L. W. Molenkamp, D. Goldhaber-Gordon and K. A. Moler, *Nature Mater.* **12**, 787 (2013).
11. V. V. Enaldiev, I. V. Zagorodnev, and V. A. Volkov, *Pis'ma v Zh. Eksp. Teor. Fiz.* **101**, 94 (2015).
12. T. L. Schmidt, S. Rachel, F. von Oppen, and L. I. Glazman, *Phys. Rev. Lett.* **108**, 156402 (2012); Nikolaos Kainaris, Igor V. Gornyi, Sam T. Carr, and Alexander D. Mirlin, *Phys. Rev. B* **90**, 075118 (2014).
13. Jukka I. Vayrynen, Moshe Goldstein, and Leonid I. Glazman, *Phys. Rev. Lett.* **110**, 216402 (2013); Jukka I. Vayrynen, Moshe Goldstein, Yuval Gefen, and Leonid I. Glazman, *Phys. Rev. B* **90**, 115309 (2014).
14. Xiao-Liang Qi, Taylor L. Hughes, and Shou-Cheng Zhang, *Nature Phys.* **4**, 273 (2008).
15. Anders Mathias Lunde and Gloria Platero, *Phys. Rev. B* **86**, 035112 (2012).
16. Z. D. Kvon, E. B. Olshanetsky, D. A. Kozlov, N. N. Mikhailov, and S. A. Dvoretsky, *Pis'ma v Zh. Eksp. Teor. Fiz.* **87**, 588 (2008).
17. E. B. Olshanetsky, Z. D. Kvon, N. N. Mikhailov, E. G. Novik, I. O. Parm, and S. A. Dvoretsky, *Sov. St. Comm.* **152**, 265 (2012).
18. Z. D. Kvon, E. B. Olshanetsky, E. G. Novik, D. A. Kozlov, N. N. Mikhailov, I. O. Parm, and S. A. Dvoretsky, *Phys. Rev. B* **83**, 193304 (2011).
19. E. B. Olshanetsky, Z. D. Kvon, Y. A. Gerasimenko, V. Prudkoglyad, V. Pudalov, N. N. Mikhailov, and S. A. Dvoretsky, *Pis'ma v Zh. Eksp. Teor. Fiz.* **98**, 947 (2013).
20. E. B. Olshanetsky, Z. D. Kvon, M. V. Entin, L. I. Magarill, N. N. Mikhailov, I. O. Parm, and S. A. Dvoretsky, *Pis'ma v Zh. Eksp. Teor. Fiz.* **89**, 338 (2009).
21. A. Kononov, S. V. Egorov, G. Biasiol, L. Sorba, and E. V. Deviatov, *Phys. Rev. B* **89**, 075312 (2014).
22. A. Kononov, S. V. Egorov, N. Titova, Z. D. Kvon, N. N. Mikhailov, S. A. Dvoretsky, and E. V. Deviatov, *Pis'ma v Zh. Eksp. Teor. Fiz.* **101**, 44 (2015).
23. A. Kononov, S. V. Egorov, Z. D. Kvon, N. N. Mikhailov, S. A. Dvoretsky, and E. V. Deviatov, *Phys. Rev. B* **93**, 041303(R) (2016).
24. D. B. Chklovskii, B. I. Shklovskii, and L. I. Glazman, *Phys. Rev. B* **46**, 4026 (1992).
25. E. Ahlswede, J. Weis, K. V. Klitzing, and K. Eberl, *Physica E* **12**, 165 (2002).
26. G. M. Gusev, Z. D. Kvon, E. B. Olshanetsky, A. D. Levin, Y. Krupko, J. C. Portal, N. N. Mikhailov, and S. A. Dvoretsky, *Phys. Rev. B* **89**, 125305 (2014).